

## Magneto-optics in GaAs-Ga<sub>1-x</sub>Al<sub>x</sub>As quantum wells

D. C. Rogers, J. Singleton, and R. J. Nicholas

*Clarendon Laboratory, Department of Physics, University of Oxford, Parks Road, Oxford OX1 3PU, England, United Kingdom*

C. T. Foxon and K. Woodbridge

*Philips Research Laboratory, Redhill, Surrey RH1 5HA, England, United Kingdom*

(Received 18 December 1985)

The interband photoconductivity of GaAs-Ga<sub>1-x</sub>Al<sub>x</sub>As quantum wells has been studied in steady fields of up to 16 T, applied both parallel and perpendicular to the growth axis. In fields parallel to the growth axis, excitonic Landau-level transitions have been identified with Landau indices up to  $n = 12$  and energies up to 400 meV above the energy gap of bulk GaAs. Transition energies and diamagnetic shifts have been measured for both allowed ( $\Delta N$  even) and forbidden ( $\Delta N$  odd) subband exciton transitions, including a transition at high energy in the widest wells which we tentatively identify as involving a bound state in the spin-orbit split-off band. Landau levels are observed at fields as low as 2.5 T, permitting a determination of exciton binding energy from linear extrapolation. High-field results are fitted using a calculation of the binding energy of two-dimensional excitons as a function of magnetic field. It is found that the exciton binding energy obtained from fitting high-field results is slightly higher than that obtained from low-field measurements, giving exciton binding energies of 16–9 meV, for well widths from 22 to 110 Å. The heavy-hole effective mass for motion in the plane of the layers is found to vary with well thickness, and this is explained by decoupling of the bands.

The study of interband optical absorption in high magnetic fields is well known to be a powerful means of band-structure determination. The technique has been applied to many bulk semiconductors [for example, GaAs (Ref. 1)] to determine basic parameters such as electron nonparabolicity and hole effective mass, and also to give detailed information on the Coulomb binding between electrons and holes. Semiconductor quantum wells formed from GaAs between Ga<sub>1-x</sub>Al<sub>x</sub>As have long been known to show strong excitonic behavior in interband spectra;<sup>2</sup> however, until recently no interband magneto-optical studies had been carried out on these systems.

Work to date on interband magnetoabsorption in quantum wells has been based on attempts to determine the exciton effective Rydberg by the extrapolation of high-field Landau levels to zero magnetic field.<sup>3,4</sup> In this work we have used results at much lower fields to estimate the exciton binding energy and a model of exciton binding in highly anisotropic systems at high magnetic fields<sup>5</sup> to deduce the band parameters of the quantum well.

The samples used were grown by molecular-beam epitaxy at Philips Research Laboratory, Redhill. Each sample consisted of a nominally undoped gallium-arsenide buffer layer grown on a semiinsulating GaAs substrate, followed by sixty periods of Ga<sub>0.65</sub>Al<sub>0.35</sub>As barriers and GaAs wells, and finally a 1300-Å Ga<sub>1-x</sub>Al<sub>x</sub>As layer. Nominal growth parameters and estimated well widths from envelope-function calculations<sup>6</sup> are given in Table I. Electrical contact to the layers was made with indium dots, alloyed at 350–400°C, and all samples were found to have resistances in the range 10<sup>5</sup>–10<sup>6</sup> Ω at room temperature. In the experiments, chopped light from a quartz halogen lamp and Czerny-Turner monochromator was

transmitted through a fiber-optic cable to the sample, which was placed in the bore of a 16 T superconducting magnet; a special insert allowed the sample to be maintained at 55–77 K in solid or liquid nitrogen. The photoconductivity of the sample, in constant current mode, was synchronously detected and recorded digitally. For experiments in magnetic fields perpendicular to the growth axis, a silvered glass prism was used to reflect the light through 90 degrees to give normal incidence to the sample face.

Figure 1 shows typical photoconductivity spectra for various different quantum-well widths at zero magnetic field. These spectra consist of a background due to interband photoconductivity in the GaAs buffer layer, with, superimposed on it, the absorption spectrum of the quantum-well layers, through which the light first passes. This technique avoids both the inconvenience of substrate removal and the optical complexity of photoluminescence measurements, and is found to give identical results.<sup>6</sup> The minima indicated are due to excitonic transitions between electron and hole subbands in the quantum well, the subbands involved being identified in Table II. These transitions include, in some cases, weak absorption edges due to free-carrier transitions between  $N=1$  subbands; these permit a direct measurement of the exciton binding energy, as will be discussed below. Table III gives subband energies in all samples as deduced from these transitions, using the method of Rogers and Nicholas,<sup>6</sup> using  $\Delta E_g = 450$  meV and the recently proposed value of  $\Delta E_c = 0.65 \Delta E_g$  (Refs. 7–11) these are all found to be bound states of the quantum wells.

Figure 2 shows spectra from the 75-Å well sample for various magnetic fields applied parallel to the growth

TABLE I. Sample well widths.

Sample	No. 1 (G50)	No. 2 (KLB155)	No. 3 (KLB205)	No. 4 (G51)	No. 5 (G55)
Well width (nominal)	25 Å	55 Å	55 Å	75 Å	125 Å
Well width (fitted)	22 Å	55 Å	60 Å	75 Å	110 Å
Barrier width (nominal)	157 Å	175 Å	175 Å	157 Å	157 Å

TABLE II. Transitions observed; zero-field energies in reduced form  $E'_T = E_T - E_g$  in meV.

Sample	No. 1	No. 2	No. 3	No. 4	No. 5
HH1- $E_1$	221	93	80	58	33
Continuum				68	
LH1- $E_1$	257	115	102	75	43
Continuum				86	52
HH2- $E_1$			123		~50
HH3- $E_1$		229	206	156	85
LH1- $E_2$		286	263	208	~120
HH2- $E_2$		312	289	221	126
LH3- $E_1$					134
LH2- $E_2$		382	356	284	167
HH4- $E_2$					~200
HH3- $E_3$					266
LH3- $E_3$					315
SO1- $E_1$				418	383

TABLE III. Calculated subband confinement energies.

Subband		Well thickness				
		22 Å	55 Å	60 Å	75 Å	110 Å
HH	$N=1$	40	19	17	13	7
	2		67	65	43	26
	3		154	142	111	59
	4					100
LH	$N=1$	76	41	38	30	17
	2		137	126	106	60
	3					109
SO	$N=1$				32	17
$E$	$N=1$	198	88	77	55	34
	2		259	244	188	108
	3					215

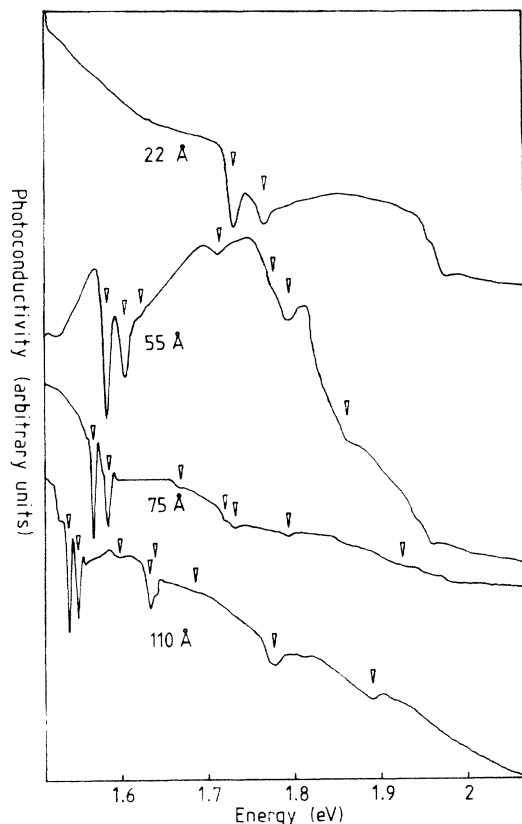


FIG. 1. Zero-magnetic-field spectra at 55 K for four different multiquantum well samples (Nos. 1, 2, 4, and 5) used in the experiments. Excitonic subband transitions are identified by arrows.

axis. When a field is applied, a series of transitions associated with Landau levels evolves from the HH1- $E_1$  exciton transition, and all the transitions previously observed at zero field are shifted up in energy proportionally to the square of the magnetic field. In Fig. 3 transition energies are plotted against magnetic field, and the evolution of Landau-level related structure can be seen clearly at low energies. Also visible at low energies is structure in between, and much weaker than, the HH1- $E_1$  structure; this arises from the Landau levels of the light-hole and electron  $N=1$  subbands. At higher energies there appears to be structure from the Landau levels of the heavy-hole and electron  $N=2$  subbands, but the complexity of the system makes quantitative conclusions very difficult. Figure 4 shows a similar diagram for the 22-Å well sample; in this case the spectra are simplified by the fact that only one bound state exists in the well for each of the three major carrier types (electrons, light holes, and heavy holes). The transition associated with the electron and heavy-hole  $n=1$  Landau levels is seen to persist to very low fields.

Previous authors<sup>3,4</sup> have interpreted the structure of magneto-optical spectra in GaAs quantum wells in terms of free-carrier inter-Landau-level transitions, of which only the  $n=1$  Landau level is subject to strong excitonic effects. This is known not to be the case in bulk GaAs,<sup>1</sup> in which Coulomb binding is significant at high fields even in the higher Landau levels. We have therefore

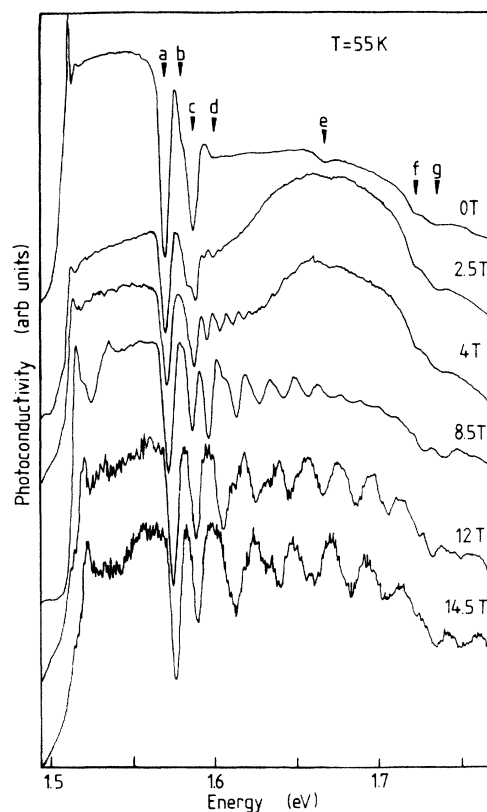


FIG. 2. Typical spectra for the 75-Å well (sample No. 4). These are high-resolution spectra over a reduced energy range, and the transitions identified are *a*, HH1- $E_1$  exciton; *b*, HH1- $E_1$  free-carrier edge; *c*, LH1- $E_1$  exciton; *d*, LH1- $E_1$  free-carrier edge; *e*, HH3- $E_1$  exciton; *f*, LH1- $E_2$  exciton; *g*, HH2- $E_2$  exciton. The forbidden LH1- $E_2$  exciton is seen to sharpen considerably at high fields.

based our analysis on the work of Akimoto and Hasegawa<sup>5</sup> for highly anisotropic systems, in which the Zeeman-shifted states of the hydrogenic exciton at low fields give rise in the high-field limit to excitonic states bound between electron and hole Landau levels.

In the limit of high magnetic field, Akimoto and Hasegawa<sup>5</sup> find the binding energy to be,

$$E_B \approx 3 \left[ \frac{\hbar e B}{2(2n+1)\mu_{exc}^* R^*} \right]^{1/2} R^* D_1, \quad (1)$$

where  $\mu_{exc}^*$  is the exciton reduced mass and  $R^*$  is the excitonic effective Rydberg.  $D_1$  is a parameter related to the dimensionality of the exciton, taking values from 0.25 (three dimensional) to 1 (two dimensional); the zero-field exciton binding energy is given by  $E_B(0) = 4R^* D_1$ .

To complete the theory we require a description of the subband dispersion relations for motion in the plane of the layers. The conduction band may be simply described by the expression, derived from  $\mathbf{k} \cdot \mathbf{p}$  perturbation theory,<sup>12</sup>

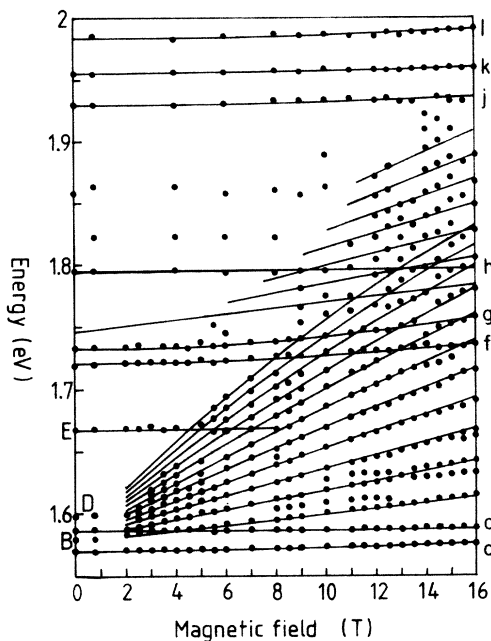


FIG. 3. Transition energies as a function of magnetic field for the 75-Å sample (No. 4). Transitions are labeled as in Fig. 2, with, additionally, *h*, LH2-E2 exciton; *j*, SO1-E1 exciton (see text); *k*, unidentified feature, appears also in samples No. 1 and No. 5 at same energy; *l*, Ga<sub>1-x</sub>Al<sub>x</sub>As band gap. The features at 1.825 and 1.86 eV do not shift systematically with field, and are thought to arise from the background due to the apparatus. The apparent downward shift of the transition *h* is an optical illusion caused by the lines crossing it.

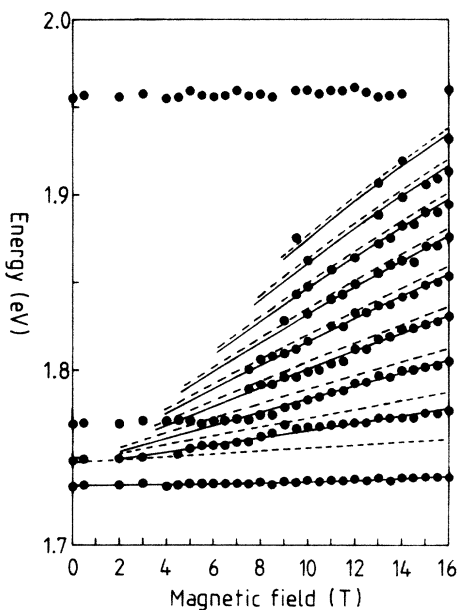


FIG. 4. Transition energies as a function of magnetic field for the 22-Å sample (No. 1). The Ga<sub>1-x</sub>Al<sub>x</sub>As band gap has been omitted, but feature *k* from Fig. 3 is seen in this diagram also. The solid lines are theoretical fits to the transition energies, as described in the text. The dashed lines represents inter-Landau-level transitions, calculated using the same parameters, to illustrate the effect of neglecting Coulomb binding.

$$E_e(B, n, K_2) = \left[ \frac{(2n+1)\hbar eB}{2m_e^*} + \frac{\hbar^2 k_z^2}{2m_e^*} \right] \times \left[ 1 + \frac{K_2}{E_g} \left[ \frac{(2n+1)\hbar eB}{2m_e^*} + \frac{\hbar^2 k_z^2}{2m_e^*} \right] \right], \quad (2)$$

where the terms in  $k_z$  arise from the quantum-well confinement, and the nonparabolicity parameter  $K_2$  describes the fourth-order contribution to the band curvature. The valence band, however, is complicated by interactions between heavy and light holes, and the subband dispersion relations do not have a simple analytic form. Expressions for the valence-band masses can, however, be derived in the limit of decoupled heavy- and light-hole bands, equivalent to the limit of high uniaxial strain, which reduces the crystal symmetry and splits the band-edge degeneracy. This limit should apply to a very narrow quantum well, which causes a similar lifting of the degeneracy. In the high-stress limit Hensel and Suzuki<sup>13</sup> have shown that the hole masses are given by

$$\frac{m_e}{m_{\perp}} = \gamma_1 - \gamma_2, \quad \frac{m_e}{m_{\parallel}} = \gamma_1 + 2\gamma_2, \quad M_j = \pm \frac{1}{2}, \quad (3)$$

$$\frac{m_e}{m_{\perp}} = \gamma_1 + \gamma_2, \quad \frac{m_e}{m_{\parallel}} = \gamma_1 - 2\gamma_2, \quad M_j = \pm \frac{3}{2},$$

for motion parallel and perpendicular to a [100] strain axis, where  $\gamma_1$  and  $\gamma_2$  are the well-known Luttinger-Kohn parameters. In a quantum well the confinement energies of the  $M_j = \pm \frac{3}{2}$  states correspond to a mass in the direction of confinement of  $(\gamma_1 - 2\gamma_2)^{-1}m_e$ ,<sup>14</sup> and are therefore commonly referred to as heavy-hole subbands; however, from (3) we see that in the limit of complete decoupling,

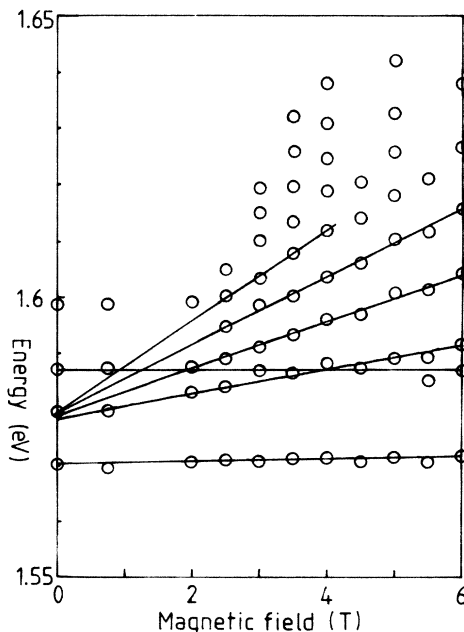


FIG. 5. Low-field, low-energy results for the 75-Å well (No. 4). Linear extrapolations of the  $N=1-4$  Landau-level transitions show the zero-field weak onset to be the exciton series limit.

TABLE IV. Measured exciton binding energies and fitted results (meV).

	Well thickness				
	22 Å	55 Å	60 Å	75 Å	100 Å
$E_B(0)$ , measured E1-HH1				10	8
E1-LH1				11	9
Fitted $E_B(0)=4R^*D_1$ (see text)	13±3	16±4	14±1	12±1	9.5±0.5

the perpendicular mass of the  $M_j = \frac{3}{2}$  state is light-hole-like, given by  $(\gamma_1 + \gamma_2)^{-1} m_e$ . This suggests that the effective mass for motion in the layer plane in the  $N=1$  heavy hole ( $M_j = \pm \frac{3}{2}$ ) subband in a GaAs quantum well will be reduced from its three-dimensional value of  $0.465 m_e$  to a value of  $0.11 m_e$  by quantum confinement, in the limit of complete decoupling. In a real system, the  $M_j$  states will not be completely decoupled, so the effective mass in this subband has been used as a variable parameter. This analogy is not adequate to describe the higher subbands, all of which will be complicated by mutual interactions.

We now discuss the interpretation of our results. The first important point is to justify the assertion that the absorption edges seen in the 75-Å well (features *b* and *d* in Fig. 2) represent the onset of free-carrier absorption. Figure 5 shows that careful extrapolation of the first Landau-level transition at low fields, where it becomes the  $2p^+$  exciton state,<sup>15</sup> gives an intersection with the zero-field axis significantly below the upper edge of the absorption onset, as does a similar extrapolation of the second Landau level, or  $3d^{2+}$ , transition. Only for the third ( $4f^{3+}$ ) and fourth ( $5g^{4+}$ ) Landau-level transitions does this difference become insignificant. It should be stressed that these extrapolations are based on data taken between 2 and 6 T, and attempts at linear extrapolation from higher fields, even based on the same transitions, give significantly higher intercept values. From our low-field results we therefore conclude that the absorption edge seen represents the series limit for excited states, and is therefore the onset of free-carrier absorption. By subtracting the energy of the appropriate exciton transition, we can therefore measure directly the exciton binding energy at zero magnetic field, and results from these measurements are included in Table IV. A similar result is included for the 110-Å sample, which shows no free-carrier onset but whose Landau levels persist at fields down to 2 T.

We next attempt to fit the experimental results using the theory described above. The adjustable parameters used are the excitonic dimensionality parameter  $D_1$  in Eq.

(1), the nonparabolicity factor  $K_2$  in Eq. (2), and the heavy-hole mass  $m_{hh}^*$  in the Landau-level expression

$$E_{hh}(B, n, m_{hh}^*) = E_0 + \frac{(2n+1)\hbar eB}{2m_{hh}^*}, \quad (4)$$

where  $E_0$  is the heavy-hole subband confinement energy. The transition energy is given by

$$E_T = E_g + E_e(B, n, K_2) + E_{hh}(B, n, m_{hh}^*) - E_B(B, n, D_1), \quad (5)$$

where the expression for  $E_B$  is corrected for electron nonparabolicity, and the parameters  $K_2$ ,  $m_{hh}^*$ , and  $D_1$  are varied to obtain the best possible fit. Best fits are shown as solid lines in Figs. 3 and 4, and can be seen to give excellent agreement at high magnetic fields. Also included in Fig. 3 is a fit to the Landau levels of the  $N=2$  heavy-hole and electron subbands, using the same band parameters as for the  $N=1$  system but a smaller exciton effective Rydberg, as suggested by Brum and Bastard.<sup>16</sup> This gives rough qualitative agreement with some of the high-field, high-energy structure. Values of fitting parameters used are given in Table V.

Table IV gives the measured values of zero-field exciton binding energy, both from fitting high-field results and from zero-field measurement and low-field extrapolation. These values are plotted against well width in Fig. 6. The fitted values from the high-field data are slightly larger than the more reliable low-field values from extrapolations made in the 75-Å and 110-Å wells; this is thought to be because measurements were taken in the intermediate-field regime, rather than the absolute high-field limit ( $\hbar\omega_c \gg R^*$ ). The values for the narrower wells show larger errors due to the fact that Landau levels in these samples can only be seen at fields above about 8 T. This highlights the need for high-quality samples, in which Landau levels can be observed at low fields, in order to make accurate extrapolations and to eliminate fitting errors.

TABLE V. Magneto-optics fitting parameters.

	Well thickness				
	22 Å	55 Å	60 Å	75 Å	110 Å
$K_2$	-1.2±0.1	-1.2±0.1	-1.2±0.1	-1.2±0.1	-1.2±0.1
$m_{hh}^* (m_e)$	-0.22±0.03	-0.47±0.06	-0.55±0.05	-0.59±0.08	-0.63±0.06
$m_{lh}^* (m_e)$				+0.25	+0.5
$D_1$ (see text)	0.67±0.16	0.79±0.21	0.69±0.05	0.60±0.05	0.48±0.03

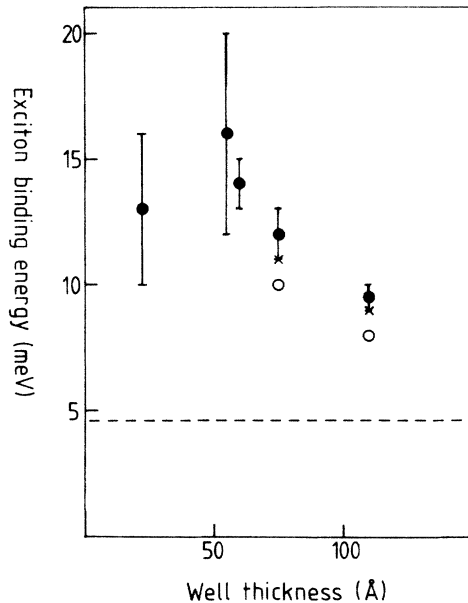


FIG. 6. Heavy-hole exciton binding energy as a function of well width for the sample studied. Results derived from high-field fits are shown as solid circles with error bars, and are systematically higher than direct measurements from low-field extrapolation, shown as open circles. Note the decrease in binding energy in the narrowest quantum well. The two diagonal crosses represent the measured light-hole binding energy. The dashed line shows the bulk exciton binding energy for GaAs.

There exists at present considerable disagreement between different methods of determining the exciton binding energy in quantum wells. Theoretical calculations<sup>17</sup> give a binding energy for the heavy-hole  $N=1$  exciton rising from the bulk value in very wide wells, to a maximum of around 10 meV at a well thickness of about 20–30 Å, and falling for narrower wells, while the light-hole  $N=1$  exciton behaves similarly except for a larger binding energy in a wide well, and a maximum value at around 30–40 Å. These are systematically lower values than the experimental results of Miller *et al.*,<sup>18</sup> who interpret the absorption edge above the exciton as a  $2s$  state, unresolved from the continuum; since a point half way up the absorption onset is chosen, this is roughly equivalent to our iden-

tification of the upper edge as the series limit, and our results are in good agreement with those of Miller *et al.* The results of Vojak *et al.*<sup>19</sup> of 13 and 20 meV, respectively, for the light- and heavy-hole exciton at zero field are estimates from an energy-level calculation based on a well width calculated from metallorganic chemical vapor deposition (MOCVD) growth rates; since such well widths are commonly incorrect by up to 10% (see, for example, Table I), these results may be subject to large errors. Finally, measurements from the magneto-optical results of Maan *et al.*<sup>3</sup> and Miura *et al.*,<sup>4</sup> give results considerably higher than theory predicts. These measurements do not take into account Coulomb effects in the higher Landau levels, which will affect the slope of the Landau-level transition as a function of field, and may also influence the determination of reduced masses by Maan *et al.*<sup>3</sup>

Also varied in the fits are the electron nonparabolicity  $K_2$  and the heavy-hole mass. We find a value for  $K_2$  of  $-1.2 \pm 0.1$  for all the wells studied; this is higher than the theoretical value, from four-band  $\mathbf{k} \cdot \mathbf{p}$  theory, of  $-0.83$  for bulk material. However,  $\mathbf{k} \cdot \mathbf{p}$  theory is known to give a good description of the GaAs conduction band,<sup>1,20</sup> so this would appear to be an effect of quantum-well confinement. The heavy-hole effective mass shows a steady decrease with decreasing well width, which is fully consistent with a progressive decoupling of the light- and heavy-hole subbands. However, the heavy-hole mass in wide wells is significantly greater than the bulk value of  $0.45m_0$ . The reduction in mass is found to offset the nonparabolicity to give a reduced mass which varies only slightly over the range of well widths studied. This is in disagreement with the results of Maan *et al.*<sup>3</sup> Reduction of the heavy-hole mass in narrow quantum wells has recently been observed in valence-band cyclotron resonance by Iwasa *et al.*,<sup>21</sup> in qualitative agreement with our results; however, they report a heavy-hole mass for wide wells equal to the bulk value.

As stated above, all the zero-field exciton transitions are observed to shift quadratically with magnetic field. The magnitudes of these shifts, where measurable, are presented in Table VI. Results for the heavy-hole  $N=1$  excitons are found to be slightly lower, and for the light-hole  $N=1$  excitons slightly higher, than those reported by Miura *et al.*;<sup>4</sup> however, the disagreement is not great. The reduced mass can be calculated from the Landau-level fits,

TABLE VI. Exciton quadratic shifts, in  $\mu\text{eV}/\text{T}^2$ . Results marked with an asterisk are subject to very large errors due to confusion with Landau-level transitions or to large linewidth.

	Well thickness				
	22 Å	55 Å	60 Å	75 Å	110 Å
HH1-E1	21	22	23	29	40
LH1-E1		5	5	13	15
HH2-E1			46		25*
HH3-E1		50*	50*	100*	
LH1-E2		40	53	65*	
HH2-E2		13	27	100*	75*
LH3-E1					85*
LH2-E2		13	18	12	
HH3-E3					59
SO1-E1				15	45*

TABLE VII. Reduced masses and dimensionality factors for HH1-E1 and LH1-E1 excitons.

	Well thickness				
	22 Å	55 Å	60 Å	75 Å	110 Å
Reduced mass ( $m_e$ )	0.062	0.064	0.065	0.064	0.062
HH1-E1					
$\Delta E_s/B^2$ ( $\mu$ eV/T <sup>2</sup> ), calculated	45	40	39	40	45
observed	21	22	23	29	40
Dimensionality parameter <sup>a</sup> $D_2$	0.47	0.55	0.59	0.73	0.89
Reduced mass ( $m_e$ )		0.105	0.108	0.084	0.086
LH1-EH1, calculated					
Light-hole mass ( $m_e$ )				+ 0.5	+ 0.4

<sup>a</sup>See text and Eq. 6.

and this gives an energy shift for the 1s state of

$$\Delta E_{1s} = D_2 \frac{\epsilon^2 \hbar^4 H^2}{4\mu^* c^2 e^2} \text{ (cgs units)}. \quad (6)$$

$D_2$  is a parameter equal to unity for a purely three-dimensional, and  $\frac{3}{16}$  for a purely two-dimensional, exciton [cf.  $D_1$  in Eq. (1)]. If we therefore put the known shift and reduced mass into (6) we obtain a value for  $D_2$ , which is again related to the dimensionality of the exciton. Assuming the light-hole exciton to behave similarly, we can obtain an estimate of the reduced mass for this exciton, and results of this calculation are presented in Table VII. In the two widest wells, Landau-level transitions calculated using this reduced mass and the measured exciton binding energy for light holes give a fairly good fit to the field dependence of the weak transitions observed in these samples. Since this reduced mass is greater than the electron mass, we conclude that the first light-hole subbands

in these wells must have electronlike dispersion relations, with a large effective mass. This is in good qualitative agreement with theoretical predictions.<sup>22</sup> The results for light-hole masses are subject to very large errors and are best taken as order-of-magnitude estimates.

It can be seen that the diamagnetic shift of the  $N=1$  heavy-hole exciton does not approach the expected two-dimensional limit ( $D_2=0.1875$ ) at small well widths; this is understandable, since the zero-thickness limit is simply the case of bulk excitons in  $\text{Ga}_{0.65}\text{Al}_{0.35}\text{As}$ . This behavior is analogous to that seen in the calculated values of exciton binding energy which peaks at around well widths of 30 Å, at an energy well below the two-dimensional limit. However, the shift in the 110-Å well is close to the three-dimensional limit, as would be expected from an exciton with a radius of about 150 Å.

In the two widest wells, the highest-energy subband transition, at 1.93 eV (75 Å) and 1.895 eV (110 Å), cannot be explained consistently with the quantum-well levels deduced from the other transitions. In the 75-Å well this transition is seen very strongly at room temperature, which suggests that it should be a  $\Delta N=0$  subband transition. We therefore tentatively identify this as the transition from the first subband of the spin-orbit split-off band to the first electron subband. Taking the spin-orbit energy in GaAs to be 341 meV, we find in both cases that the confinement energy of the split-off hole subband is close to that of the first light-hole subband, as would be expected from their similar effective masses. This will be discussed in more detail in a forthcoming paper.<sup>23</sup>

Finally, spectra were also taken with magnetic field applied perpendicular to the growth axis. Typical results are shown in Fig. 7, for the 60-Å well sample. No change was observed in the  $N=1$  subband energies in any well studied. A slight shift was observed in some higher transitions, but in every case the line width was too great to make any reliable measurement.

In conclusion, we have obtained, from a study of the magneto-optics of quantum wells, detailed results concerning the subband structure of all three major carrier types. The conduction-band nonparabolicity is enhanced by quantum confinement; the heavy-hole effective mass for motion in the layer plane decreases considerably for decreasingly well widths, and the light hole exhibits elec-

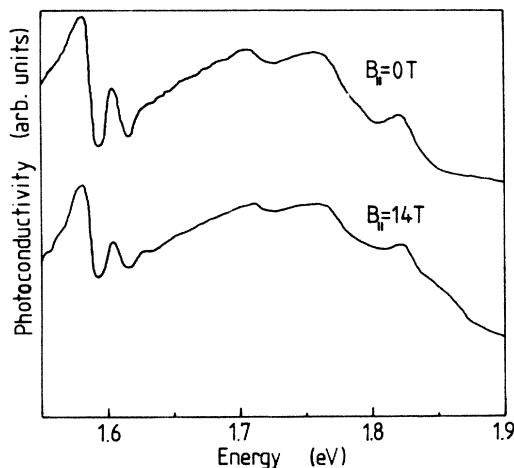


FIG. 7. Spectra of the 60-Å sample (No. 3) with magnetic field perpendicular to the growth axis. No significant change is seen in any of the major features.

tronlike motion in the layer plane. We have also analyzed the binding of excitons as a function of Landau level and magnetic field, and shown that a magneto-optical determination of the zero-field exciton binding energy gives good agreement with zero-field measurements of this energy. The exciton binding energy is found to be  $(9 \pm 1)$  meV in a 110-Å well, rising to  $(16 \pm 4)$  eV in a 55-Å well, and becoming smaller  $(13 \pm 3)$  meV in a 22-Å well, in qualitative agreement with theoretical calculations. For narrow wells these results are still significantly greater than would be predicted by current theories.

*Note added in proof.* The availability of a new, higher quality GaAs-Ga<sub>1-x</sub>Al<sub>x</sub>As multiple quantum well sample, with ~60-Å well width, has enabled us to deduce HH1-E1 and LH1-E1 exciton binding energies of  $12.5 \pm 1$  meV and  $13.5 \pm 1$  meV, respectively, using the low-field extrapolation technique, in reasonable agreement with the fitted values reported above. In addition, recent pump

and probe cyclotron resonance experiments performed on the samples described in this paper, have indicated that the electron nonparabolicity due to motion in the plane of the well (cyclotron motion) is much larger than that due to confinement. A model which includes these features and which reproduces the electron effective masses observed in the cyclotron resonance data has been formulated, and has been used to fit the interband magneto-optical data presented in this paper: the fitted high-field exciton binding energies used are much closer to the directly measured values. These values will be published in the near future.<sup>24</sup>

#### ACKNOWLEDGMENTS

We would like to thank Dr. G. Duggan and Dr. H. I. Ralph for useful discussions.

- 
- <sup>1</sup>Q. H. F. Vreken, *J. Phys. Chem. Solids* **29**, 129 (1968).  
<sup>2</sup>R. Dingle, W. Weigmann, and C. H. Henry, *Phys. Rev. Lett.* **33**, 827 (1974).  
<sup>3</sup>J. C. Maan, G. Belle, A. Fasolino, M. Altarelli, and K. Ploog, *Phys. Rev. B* **30**, 2253 (1984).  
<sup>4</sup>N. Miura, Y. Iwasa, S. Tarucha, and H. Okamoto, in *Proceedings of the 17th International Conference Physics of Semiconductors*, edited by J. D. Chadi and W. A. Harrison (Springer, New York, 1984), p. 359.  
<sup>5</sup>O. Akimoto and H. Hasegawa, *J. Phys. Soc. Jpn.* **22**, 181 (1967).  
<sup>6</sup>D. C. Rogers and R. J. Nicholas, *J. Phys. C* **18**, L891 (1985).  
<sup>7</sup>R. C. Miller, A. C. Gossard, D. A. Kleinmann, and O. Munteanu, *Phys. Rev. B* **29**, 3740 (1984).  
<sup>8</sup>W. I. Wang, E. E. Mendez, and F. Stern, *Appl. Phys. Lett.* **45**, 639 (1984).  
<sup>9</sup>J. Batey, S. L. Wright, and D. J. Dimaria, *J. Appl. Phys.* **57**, 484 (1985).  
<sup>10</sup>M. H. Meynardier, C. Delalande, G. Bastard, M. Voos, F. Alexandre, and J. L. Lievin, *Phys. Rev. B* **31**, 5539 (1985).  
<sup>11</sup>G. Duggan, H. I. Ralph, and K. J. Moore, *Phys. Rev. B* **32**, 8395 (1985).  
<sup>12</sup>E. D. Palik, G. S. Picus, S. Teitler, and R. F. Wallis, *Phys. Rev.* **122**, 475 (1961).  
<sup>13</sup>J. C. Hensel and K. Suzuki, *Phys. Rev. B* **9**, 4219 (1974).  
<sup>14</sup>G. Bastard, *Phys. Rev. B* **24**, 5693 (1981).  
<sup>15</sup>P. J. Lin-Chung and B. W. Henvis, *Phys. Rev. B* **12**, 630 (1975).  
<sup>16</sup>J. A. Brum and G. Bastard, *J. Phys. C* **18**, L789 (1985).  
<sup>17</sup>K. S. Chan, *J. Phys. C* **19**, L125 (1986).  
<sup>18</sup>R. C. Miller, D. A. Kleinmann, W. T. Tsang, and A. C. Gossard, *Phys. Rev. B* **24**, 1134 (1981).  
<sup>19</sup>B. A. Vojak, N. Holonyak, Jr., D. W. Laidig, K. Hess, J. J. Coleman, and P. D. Dapkus, *Solid State Commun.* **35**, 477 (1980).  
<sup>20</sup>G. Lindemann, R. Lassnig, W. Seidenbusch, and E. Gornik, *Phys. Rev. B* **28**, 4693 (1983).  
<sup>21</sup>Y. Iwasa, N. Miura, S. Tarucha, H. Okamoto, and T. Ando, *Surf. Sci.* **170**, 587 (1986).  
<sup>22</sup>G. D. Sanders and Y. C. Chang, *Phys. Rev. B* **31**, 6892 (1985).  
<sup>23</sup>G. Duggan, H. I. Ralph, P. Dawson, K. Moore, J. Singleton, R. J. Nicholas, D. C. Rogers, and C. T. Foxon (unpublished).  
<sup>24</sup>J. Singleton, R. J. Nicholas, D. C. Rogers, and C. T. B. Foxon in *Proceedings of the Application of High Magnetic Fields in Semiconductor Physics, Würzburg* (Springer, Berlin, 1986), and to be published.